High current densities in a highly photoluminescent organic single-crystal light-emitting transistor

Sawabe, Kosuke; Takenobu, Taishi; Bisri, Satria Zulkarnaen; Yamao, Takeshi; Hotta, Shu; Iwasa, Yoshihiro

Published in:
Applied Physics Letters

DOI:
10.1063/1.3466915

Publication date:
2010

High current densities in a highly photoluminescent organic single-crystal light-emitting transistor

Kosuke Sawabe, Taishi Takenobu, Satria Zulkarnaen Bisri, Takeshi Yamao, Shu Hotta, and Yoshihiro Iwasa

Citation: Appl. Phys. Lett. **97**, 043307 (2010); doi: 10.1063/1.3466915
View online: https://doi.org/10.1063/1.3466915
View Table of Contents: http://aip.scitation.org/toc/apl/97/4
Published by the American Institute of Physics

High current densities in a highly photoluminescent organic single-crystal light-emitting transistor

Kosuke Sawabe,[1] Taishi Takenobu,[2,3,a)] Satria Zulkarnaen Bisri,[1] Takeshi Yamao,[4] Shu Hotta,[4] and Yoshihiro Iwasa[5,6]
[1]*Department of Physics, Graduate School of Science, Tohoku University, Sendai 980-8578, Japan*
[2]*Department of Applied Physics, Graduate School of Advanced Science and Engineering, Waseda University, Tokyo 169-8555, Japan*
[3]*PRESTO, Japan Science and Technology Agency (JST), Saitama 332-0012, Japan*
[4]*Department of Macromolecular Science and Engineering, Kyoto Institute of Technology, Kyoto 606-8585, Japan*
[5]*Quantum-Phase Electronic Center, School of Engineering, The University of Tokyo, Tokyo 113-8656, Japan*
[6]*CREST, Japan Science and Technology Agency (JST), Saitama 332-0012, Japan*

(Received 24 May 2010; accepted 28 June 2010; published online 30 July 2010)

We report the improvement of electron transport in 5,5″-bis(biphenylyl)-2,2′:5′,2″-terthiophene (BP3T) single crystals on a field-effect transistor configuration by systematically investigating the effects of device aging under pure nitrogen and optimizing the organic dielectric layer-fabrication process. We reduced the effect of electron traps and achieved extremely high current densities up to 10 kA/cm^2, which is one or two orders of magnitude greater than the current densities achieved in previous devices. © *2010 American Institute of Physics*. [doi:10.1063/1.3466915]

Several advances in organic material science have accelerated the development of organic devices such as light-emitting diodes (LEDs), field-effect transistors (FETs) and photovoltaic cells.[1–3] Organic LED-based displays and lighting fixtures are already released to the market. While there has been rapid progress in developing organic light-emitting devices, important questions still remain regarding organic lasers. Although amplified spontaneous emission (ASE) and lasing from optically pumped organic thin films and single crystals have been observed for over a decade, electrically driven organic lasers have not yet been achieved.[4–6]

A conventional approach to electrically driven lasing was attempted using an LED structure[7,8] but it had several drawbacks that were largely related to the low carrier mobilities of organic materials and thin films. Because of low mobility, it is difficult to pass very high current densities through most organic semiconductor thin-film devices. In addition, it is difficult to move contacts far from the recombination zone although they are a source of optical loss.

In addition to conventional organic LED devices, organic light-emitting field-effect transistors (LETs) have been developed.[9–11] Organic single-crystal LETs (OSCLETs) with ambipolar charge transport are suitable for laser devices because they offer a high carrier mobility and a geometry that minimizes the effects of nonradiative losses.[12,13] In tetracene and rubrene, the maximum current density of ambipolar OSCLETs can reach several kA/cm^2 (assuming 1 nm thick accumulation layer) without degradation of the external quantum efficiency.[14] Interestingly, in 5,5″-bis(biphenylyl)-2,2′:5′,2″-terthiophene (BP3T) OSCLETs, a current density-dependent spectral evolution was detected, possibly indicating an initial stage of ASE—although no clear threshold behavior has yet been observed.[8,15] To achieve further spectral evolution and definitively detect electrically-driven ASE, the current density must be increased.

In this paper, we achieved an extremely high current density in BP3T single crystal-based ambipolar organic LETs. Single-crystal BP3T is a promising material for laser devices because laser oscillation under photoexcitation[16,17] and current-driven spectral evolution in ambipolar LETs (Ref. 15) have been observed. However, the electron mobility (~0.1 $cm^2/V\,s$) is far less than the hole mobility (>1 $cm^2/V\,s$), and the electron threshold voltage (~150 V) is much higher than that of the hole threshold voltage (~−30 V) in BP3T OSCLETs. These results clearly suggest the presence of a large number of electron traps in present devices and much room for improvement. To enhance the electron transport characteristics of BP3T LETs, we tried to remove electron traps by adopting two different methods: aging the device inside an N_2-filled glove box, the effectiveness of which has been demonstrated in rubrene single-crystal ambipolar transistors,[18] and optimizing the fabrication process for the organic polymer dielectric layers. Using these methods, we have achieved extremely high current densities (up to 10 kA/cm^2).

LETs based on BP3T single crystals were fabricated using a well-established method for ambipolar organic single-crystal FETs.[15,19–21] A highly doped silicon wafer with a 500 nm thermally oxidized SiO_2 layer was spin-coated with poly(methyl methacrylate) (PMMA) (Sigma-Aldrich Co., average M_w ~ 120 000). The substrate was heated at 70 °C for 6 h and then annealed at 110 °C for 3 h. These temperatures were selected based on the glass transition temperature (105 °C) and the melting temperature (130 °C) of PMMA. Single crystals of BP3T were grown by physical vapor transport under an Ar gas stream.[22] These crystals were transferred into the glove box without exposure to air and laminated onto the PMMA/SiO_2/Si substrates. Au and Ca were used for the source and drain electrodes to reduce the injection barrier for both the hole and electron carriers [Figs. 1(a) and 1(b)]. Electrical characterization of the device was performed inside the glove box in the dark via a semiconducting parameter analyzer.

a)Electronic mail: takenobu@waseda.jp.

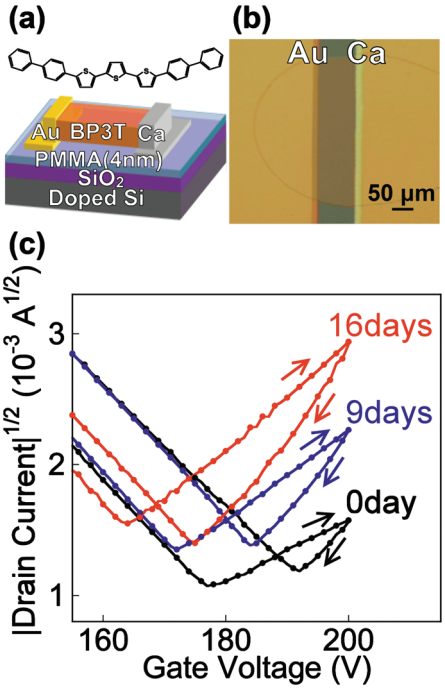

FIG. 1. (Color) (a) Schematic representation of a BP3T molecule (see Ref. 23) and single-crystal transistor. (b) Photograph of a BP3T single-crystal transistor. (c) Nitrogen atmosphere aging time dependence of transfer characteristics. Black, blue, and red lines correspond to the characteristics of the as-fabricated device, the device after 9 days, and the device after 16 days, respectively.

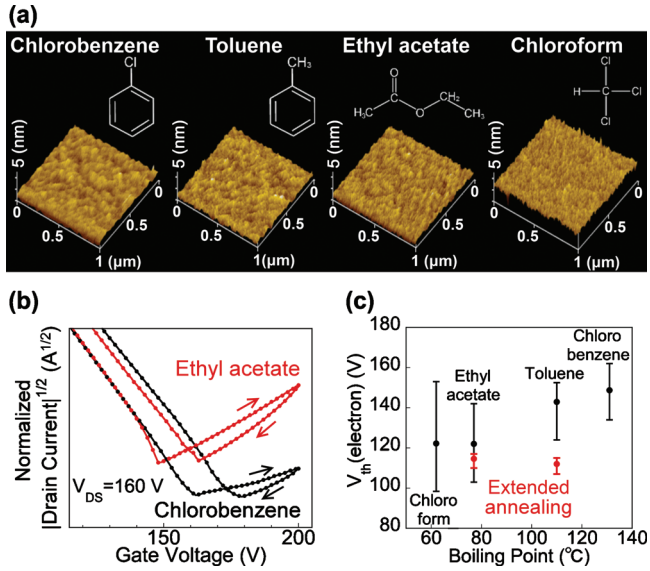

FIG. 2. (Color) (a) AFM profile images of the PMMA surfaces fabricated by chlorobenzene, toluene, ethyl-acetate, and chloroform solutions, respectively. (b) Transfer characteristics of BP3T ambipolar transistors with spin-coated PMMA layers from chlorobenzene (black) and ethyl-acetate (red) solutions. (c) The observed relationship between the electron threshold voltage and the solvent boiling points. Red markers represent the result after extended heating (one week in total).

We adopted two different methods to reduce the effect of electron traps. The effect of aging the device under nitrogen was investigated because its effectiveness had already been demonstrated for rubrene single-crystal ambipolar transistors.[18] In the rubrene transistors, both an electron-mobility enhancement and a decrease in electron threshold voltage were observed. The most likely origin of these effects is the desorption of ambient air (oxygen and/or water). We kept the BP3T devices inside the N_2-filled glove box and repeatedly measured the electrical characteristics (at arbitrary times) to observe the improvement of electron transport. Figure 1(c) shows the time dependence of the n-channel transfer characteristics of the device with the best performance. After 16 days of aging, the electron mobility reached 0.11 $cm^2/V\,s$ for the forward sweep and 0.27 $cm^2/V\,s$ for the backward sweep—the highest electron mobility reported for BP3T transistors.[15] We repeatedly observed the gradual enhancement of the n-channel characteristics in all (more than ten) of the tested devices. Because device aging under nitrogen is a very mild treatment, the desorption of ambient air might be the origin of this effect.[18,24,25]

We then focused on the PMMA buffer layers. In particular, we hypothesized that one of the possible origins of electron traps could be residual solvent molecules in the PMMA films because the boiling point of toluene, our solvent, was identical to the annealing temperature (110 °C). To clarify the influence of the solvent, we prepared PMMA layers using chlorobenzene, toluene, ethyl-acetate, and chloroform and fabricated BP3T single-crystal transistors. Figure 2(a) shows atomic force microscopy (AFM) profile images of spin-coated PMMA films. The observed surface morphologies of these films were equally smooth and the root mean square values of the surface roughness are similar for the four solvents; 0.17 nm for chlorobenzene, 0.19 nm for toluene, 0.19 nm for ethyl acetate, and 0.28 nm for chloroform. Despite the almost-identical surface morphologies, we observed considerable differences in the electron transport properties. Figure 2(b) shows the typical solvent dependence of the n-channel transfer characteristics. A clear contrast was observed between the BP3T ambipolar FETs that used PMMA buffer layers made from ethyl acetate and chlorobenzene solutions. We fabricated more than five devices for each solvent to statistically confirm these differences, and we found an obvious relationship between the electron threshold voltage and the solvent boiling point [Fig. 2(c) black dots]. This result strongly indicates the effect of residual solvent because a higher boiling point leads to a higher number of remaining solvent molecules in the PMMA film. These residual molecules could be the origin of electron traps.

To remove solvent molecules completely, we extended the heating time from 9 h (70 °C for 6 h, then 110 °C for 3 h) to 7 days (70 °C for 2 days, then 110 °C for 5 days) for the toluene- and ethyl-acetate-based PMMA films. The corresponding electron transport parameters are plotted in Fig. 2(c) as red dots. The threshold voltages became very similar between the two solvents with small error bars, strongly suggesting the removal of electron traps. These results led us to conclude that residual solvent is one of the origins of electron traps and can be removed through extended annealing. The electron-trapping mechanism, however, is still unknown. Inhomogeneity of the dielectric constant inside PMMA films resulting from the residual polar solvent molecules is one possible cause, as it is well known that the carrier mobility is dependent on the gate dielectric constant.[26–28] Structural disorder due to residual molecules produces a similar effect, and direct carrier trapping by the molecular orbitals of solvent molecules is another possible cause. A different interpretation of this effect is the rearrangement of the PMMA layer by extended annealing. It should be noted that the electron threshold voltage remained high after extended annealing,

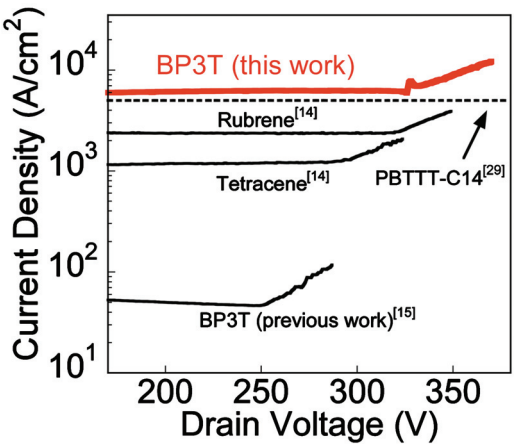

FIG. 3. (Color) (a) Scaled output characteristics of various organic single-crystal FETs under ambipolar operation. The maximum current density of PBTTT-C14:poly(2,5-bis(3-tetradecylthiophen-2-yl)thieno[3,2-b]thiophene), assuming a 1 nm thick accumulation layer, is plotted with the dashed line.

indicating the existence of another type electron trap.

A high ambipolar current density (>10 kA/cm^2, by assuming 1 nm accumulation layer thickness) was achieved, owing to the improvements in the electron transport characteristics described above. Figure 3 shows the output characteristics of the BP3T single-crystal device and various other organic single-crystal FETs.[14,15] The constant drain current corresponds to a hole-saturation current, and the steep current increase at the higher drain bias represents the onset of electron transport. In each device, the maximum drain current consists of both hole and electron currents with a ratio of nearly 1:1, which is necessary for high recombination efficiency. To make a fair comparison of the current density with previous reports, we have adopted the assumption of a 1 nm thick accumulation layer for all reported results. In our previous BP3T device,[15] the maximum current density reached was less than 0.5 kA/cm^2 due to the limited electron current. Moreover, the reported maximum current densities for thin-film and single-crystal ambipolar LETs were 5 kA/cm^2 (originally 2.5 kA/cm^2, assuming a 2 nm thickness)[29] and 4 kA/cm^2 (originally 0.4 kA/cm^2, assuming a 10 nm thickness),[14] respectively. In this study, the improved electron transport characteristics enabled us to inject higher current and, for the best-performing device, a current density up to 12.3 kA/cm^2 was achieved.

We should discuss the current density required for electrical driven lasing. In the previous paper,[15] we have estimated the necessary current density for BP3T single crystals from the photopumped ASE threshold energy[16] and the room temperature exciton lifetime.[30] The estimated threshold current density was 10.3 kA/cm^2 and this is reachable value for our best devices. However, this estimation neglected the possible threshold increase due to the metal electrodes,[31] polarons,[32] and exciton annihilation,[33] and the necessary current density must be much higher than the value of this calculation. Therefore, we need to continue our efforts to improve current density because there is still another type of electron traps in ore devices. In addition, we should reduce the necessary current density using cavity effects.

In conclusion, the electron transport characteristics were improved by device aging in an inert atmosphere and the optimization of the PMMA solvent. The maximum ambipolar current density achieved was 12.3 kA/cm^2, which is one or two orders of magnitude larger than the current density achieved in previous devices. The achievement of an extremely high current density will likely extend the performance limits of single-crystal light-emitting transistors and open a realistic route for electrically driven organic lasers.

This study was partially supported by a Grant-in-Aid from MEXT, Japan (Grant Nos. 17069003 and 22656003).

[1] R. H. Friend, R. W. Gymer, A. B. Holmes, J. H. Burroughes, R. N. Marks, C. Taliani, D. D. C. Bradley, D. A. Dos Santos, J. L. Bredas, M. Logdlund, and W. R. Salaneck, Nature (London) **397**, 121 (1999).
[2] C. D. Dimitrakopoulos and P. R. L. Malenfant, Adv. Mater. **14**, 99 (2002).
[3] R. W. I. de Boer, M. E. Gershenson, A. F. Morpurgo, and V. Podzorov, Phys. Status Solidi A **201**, 1302 (2004).
[4] I. D. W. Samuel and G. A. Turnbull, Chem. Rev. (Washington, D.C.) **107**, 1272 (2007).
[5] H. Yamamoto, T. Oyamada, H. Sasabe, and C. Adachi, Appl. Phys. Lett. **84**, 1401 (2004).
[6] M. Ichikawa, R. Hibino, M. Inoue, T. Haritani, S. Hotta, T. Koyama, and Y. Taniguchi, Adv. Mater. **15**, 213 (2003).
[7] L. S. Hung and C. H. Chen, Mater. Sci. Eng. R. **39**, 143 (2002).
[8] I. D. W. Samuel, E. B. Namdas, and G. A. Turnbull, Nat. Photonics **3**, 546 (2009).
[9] A. Hepp, H. Heil, W. Weise, M. Ahles, R. Schmechel, and H. von Seggern, Phys. Rev. Lett. **91**, 157406 (2003).
[10] J. Zaumseil, R. H. Friend, and H. Sirringhaus, Nature Mater. **5**, 69 (2006).
[11] M. Muccini, Nature Mater. **5**, 605 (2006).
[12] T. Takahashi, T. Takenobu, J. Takeya, and Y. Iwasa, Adv. Funct. Mater. **17**, 1623 (2007).
[13] H. Nakanotani, M. Saito, H. Nakamura, and C. Adachi, Appl. Phys. Lett. **95**, 033308 (2009).
[14] T. Takenobu, S. Z. Bisri, T. Takahashi, M. Yahiro, C. Adachi, and Y. Iwasa, Phys. Rev. Lett. **100**, 066601 (2008).
[15] S. Z. Bisri, T. Takenobu, Y. Yomogida, H. Shimotani, T. Yamao, S. Hotta, and Y. Iwasa, Adv. Funct. Mater. **19**, 1728 (2009).
[16] M. Ichikawa, K. Nakamura, M. Inoue, H. Mishima, T. Haritani, R. Hibino, T. Koyama, and Y. Taniguchi, Appl. Phys. Lett. **87**, 221113 (2005).
[17] N. Matsuoka, T. Hiramatsu, H. Yanagi, F. Sasaki, and S. Hotta, Phys. Status Solidi C **6**, 338 (2009).
[18] S. Z. Bisri, T. Takenobu, T. Takahashi, and Y. Iwasa, Appl. Phys. Lett. **96**, 183304 (2010).
[19] T. Takahashi, T. Takenobu, J. Takeya, and Y. Iwasa, Appl. Phys. Lett. **88**, 033505 (2006).
[20] T. Takenobu, T. Takahashi, J. Takeya, and Y. Iwasa, Appl. Phys. Lett. **90**, 013507 (2007).
[21] S. Z. Bisri, T. Takahashi, T. Takenobu, M. Yahiro, C. Adachi, and Y. Iwasa, Jpn. J. Appl. Phys., Part 2 **46**, L596 (2007).
[22] R. A. Laudise, C. Kloc, P. G. Simpkins, and T. Siegrist, J. Cryst. Growth **187**, 449 (1998).
[23] S. Hotta, H. Kimura, S. A. Lee, and T. Tamaki, J. Heterocycl. Chem. **37**, 281 (2000).
[24] A. J. Maliakal, J. Y. C. Chen, W. Y. So, S. Jockusch, B. Kim, M. F. Ottaviani, A. Modelli, N. J. Turro, C. Nuckolls, and A. P. Ramirez, Chem. Mater. **21**, 5519 (2009).
[25] T. Kaji, T. Takenobu, A. F. Morpurgo, and Y. Iwasa, Adv. Mater. **21**, 3689 (2009).
[26] I. N. Hulea, S. Fratini, H. Xie, C. L. Mulder, N. N. Iossad, G. Rastelli, S. Ciuchi, and A. F. Morpurgo, Nature Mater. **5**, 982 (2006).
[27] J. Veres, S. D. Ogier, S. W. Leeming, D. C. Cupertino, and S. M. Khaffaf, Adv. Funct. Mater. **13**, 199 (2003).
[28] A. F. Stassen, R. W. I. de Boer, N. N. Iosad, and A. F. Morpurgo, Appl. Phys. Lett. **85**, 3899 (2004).
[29] E. B. Namdas, P. Ledochowitsch, J. D. Yuen, D. Moses, and A. J. Heeger, Appl. Phys. Lett. **92**, 183304 (2008).
[30] S. Kanazawa, M. Ichikawa, T. Koyama, Y. Taniguchi, and S. Hotta, ChemPhysChem **7**, 1881 (2006).
[31] M. A. Baldo, R. J. Holmes, and S. R. Forrest, Phys. Rev. B **66**, 035321 (2002).
[32] T. Rabe, P. Gorrn, M. Lehnhardt, M. Tilgner, T. Riedl, and W. Kowelsky, Phys. Rev. Lett. **102**, 137401 (2009).
[33] C. Gärtner, C. Karnutsch, U. Lemmer, and C. Pflumm, J. Appl. Phys. **101**, 023107 (2007).